Bio-Design and Manufacturing (2021) 4:842–850
https://doi.org/10.1007/s42242-021-00141-8

RESEARCH ARTICLE

# Porous hydrogel arrays for hepatoma cell spheroid formation and drug resistance investigation

Xin Lei[1] · Changmin Shao[1,2] · Xin Shou[2,3] · Keqing Shi[1] · Liang Shi[4] · Yuanjin Zhao[1,2,3]

Received: 24 February 2021 / Accepted: 4 June 2021 / Published online: 17 July 2021


## Abstract

Drug resistance is one of the major obstacles in the drug therapy of cancers. Efforts in this area in pre-clinical research have focused on developing novel platforms to evaluate and decrease drug resistance. In this paper, inspired by the structure of hives where swarms live and breed, we propose porous hydrogel arrays with a uniform pore structure for the generation of hepatoma cell spheroids and the investigation of drug resistance. The porous hydrogel arrays were fabricated using polyethylene glycol diacrylate (PEGDA) hydrogel to negatively replicate a well-designed template. Benefiting from the elaborate processing of the template, the prepared porous hydrogel arrays possessed a uniform pore structure. Due to their anti-adhesion properties and the excellent biocompatibility of the PEGDA hydrogel, the hepatoma cells could form well-defined and uniform hepatoma cell spheroids in the porous hydrogel arrays. We found that the resistant hepatoma cell spheroids showed more significant Lenvatinib resistance and a migratory phenotype compared with a two-dimensional (2D) cell culture, which reveals the reason for the failure of most 2D cell-selected drugs for in vivo applications. These features give such porous hydrogel arrays promising application prospects in the investigation of tumor cell spheroid culture and in vitro drug resistance.

**Keywords** Drug resistance · Hydrogel · Porous · Spheroid · Hepatoma

## Introduction

Drug resistance has always been a principal impediment affecting the overall survival and prognosis of cancer patients [1–4]. Despite great progress being made in tumor treatment, the problem is still widespread and has made efforts to combat drug resistance a major focus [5–8]. In order to improve responsiveness to chemotherapeutic drug treatments, numerous in vitro models and platforms have been developed for drug resistance research, such as two-dimensional (2D) cell cultures and animal studies [9–12]. Although a conventional 2D cell culture model can elucidate the molecular and cellular mechanisms of drug resistance and provide a basis for targeted therapy, it cannot reflect the actual effect of drugs in vivo because it is difficult for the 2D cell culture model to accurately simulate the complex cell–cell and cell–matrix interactions in solid tumors [13–15]. In addition, due to species differences, high costs, technical complexity, and ethical issues, the application of animal models is also largely restricted [16–18]. Thus, the development of a new in vitro model for drug resistance investigation that can solve the shortcomings of the above two traditional models is still highly anticipated.

In this paper, inspired by the structure of hives where swarms live and breed, we present new porous hydrogel arrays with desirable features for tumor cell spheroid formation and drug resistance investigation, as illustrated in Fig. 1. As a typical three-dimensional (3D) cell culture model, the tumor cell spheroid culture is a promising approach for obtaining and maintaining the functional

✉ Changmin Shao
shaocm@wiucas.ac.cn

✉ Liang Shi
shiliang3@mail.sysu.edu.cn

✉ Yuanjin Zhao
yjzhao@seu.edu.cn

1 Translational Medicine Laboratory, The First Affiliated Hospital of Wenzhou Medical University, Wenzhou 325035, China

2 Wenzhou Institute, University of Chinese Academy of Sciences, Wenzhou 325001, China

3 State Key Laboratory of Bioelectronics, School of Biological Science and Medical Engineering, Southeast University, Nanjing 210096, China

4 Department of Laboratory Medicine, The Eighth Affiliated Hospital, Sun Yat-Sen University, Shenzhen 518033, China

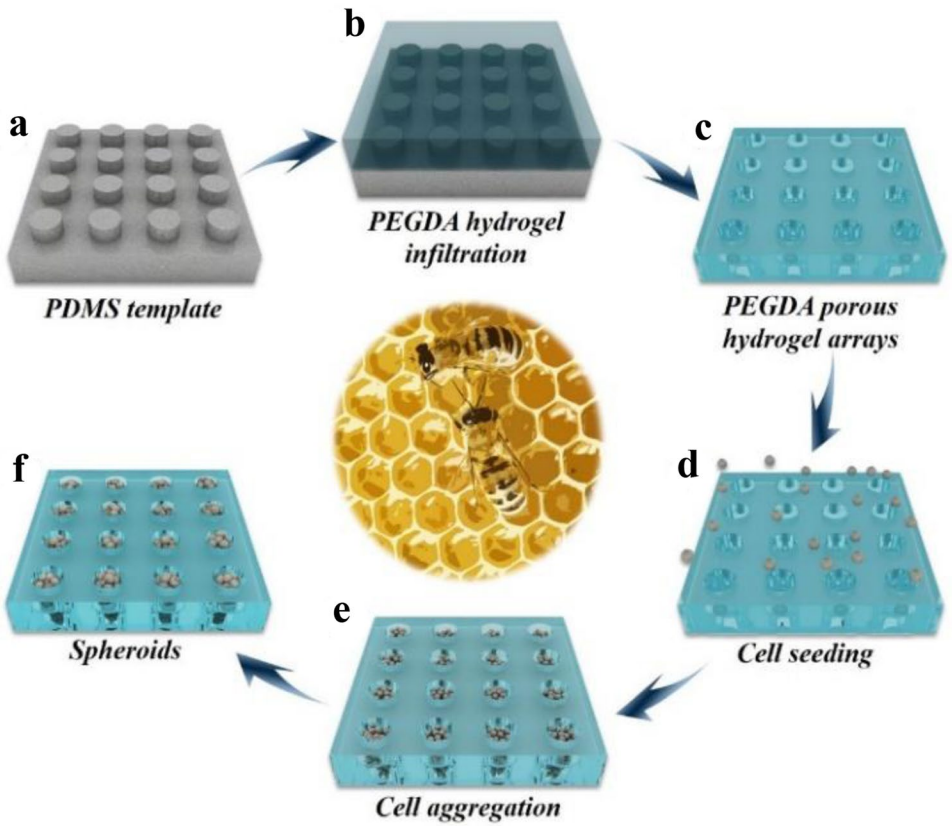


**Fig. 1** Illustration of the porous hydrogel arrays for cell spheroid formation: **a–c** fabrication of PEGDA porous hydrogel arrays, **d–f** cell spheroid formation

phenotypes of tumor cells in vitro [19, 20]. Because tumor cell spheroids can better simulate and reconstruct the morphological, functional, and microenvironmental characteristics of solid tumors in vitro, they have been widely applied in cancer research, especially for the development and screening of anti-tumor drugs [21, 22]. To achieve the formation of such spheroids, a large number of 3D culture methods have been developed, such as hydrogel embedding, 3D scaffolds, hanging drops, non-adherent surfaces, rotating culture, microfluidic technology [23, 24]. Although there has been much progress, there are still many defects in these methods—such as their complex operation, low throughput, uncontrollable sphere size, and uncertain biocompatibility—which greatly limit their practical application [25, 26]. In addition, the use of these tumor cell spheroids for the investigation of drug resistance is rare, and the systematic, comparative study of 2D and 3D models remains an unexplored area.

In this paper, we employ a simple template replication approach for the generation of hive-like porous hydrogel arrays for hepatoma cell spheroid formation and the related resistance investigation. Because of their excellent biomimetic microenvironment, hydrogels have been widely designed to culture cells in a 3D manner [27, 28]. Thus, polyethylene glycol diacrylate (PEGDA) hydrogel was selected here to generate porous arrays for hepatoma cell spheroid culture due to its strong biocompatibility and anti-adhesion properties. The fabricated porous hydrogel arrays had a uniform pore structure, which was inherited from the precise template of micro–nanoprocessing. It was demonstrated that the hepatoma cells could produce a large number of uniform hepatoma cell spheroids in the porous hydrogel arrays. Based on this, we found that the resistant hepatoma cell spheroids showed more remarkable Lenvatinib resistance and migratory phenotype compared with a 2D cell culture. This shows the reason for the failure of most 2D cell-selected drugs for in vivo applications. Thus, we believe that our porous hydrogel arrays can serve as a simple tool for culturing tumor cell spheroids and in in vitro drug resistance investigation.

## Materials and methods

### Materials

A polydimethylsiloxane (PDMS) microcolumn template was customized from Taizhou Weikai Biotechnology Co., Ltd, China. Lenvatinib (E7080) was purchased from MCE, Shanghai, China. The Huh7 cells were obtained from the Procell, Wuhan, China, and the Lenvatinib-resistant cell line (Huh7R cells) was established in our laboratory.

Poly(ethylene glycol) diacrylate (PEGDA, average molecular weight of 700), 2-hydroxy-2-methylpropiophenone (HMPP), dimethyl sulfoxide (DMSO), 3-(4,5-dimethylthiazol-2-yl)-2,5-diphenyltetrazolium bromide (MTT) powder and a phosphatase inhibitor cocktail were purchased from Sigma-Aldrich, USA. Calcein-AM, propidium iodide (PI), and an enhanced chemiluminescence (ECL) reagent were purchased from Thermo Fisher Scientific, USA. Cell Counting Kit-8 (CCK8) was bought from Dojindo Laboratories, Kumamoto, Japan. Dulbecco's modified Eagle's medium (DMEM), penicillin-streptomycin double antibiotics, phosphate-buffered saline (PBS), and trypsin were purchased from Gibco, Grand Island, NY, USA. Fetal bovine serum (FBS) was obtained from Lonsera, Shanghai, China. A radio immunoprecipitation assay (RIPA) buffer, bicinchoninic acid (BCA), protein assay kit, and a secondary antibody were purchased from Beyotime, Shanghai, China. 1,4-Dithiothreitol (DTT), sodium dodecyl sulfate (SDS), 30% polyacrylamide gel electrophoresis (PAGE), paraformaldehyde, crystal violet, and Tris-buffered saline with Tween 20 (TBST) were obtained from Solarbio, Beijing, China. The protease inhibitor was purchased from Roche, Indianapolis, IN, USA. Transwell chambers (Costar #3422) were bought from Corning, NY, USA. Polyvinylidene fluoride (PVDF) membrane was obtained from Millipore, Bedford, USA. Primary antibodies were the GAPDH antibody (1:5000, Proteintech, Wuhan, China), P-glycoprotein (P-gp) antibody (1:2000, Abcam, UK), E-cadherin antibody (1:2000, Cell Signaling Technology, Danvers, MA, USA), and Vimentin antibody (1:2500, Cell Signaling Technology, Danvers, MA, USA). All other reagents were commercially purchased and of the best available grade.

## Fabrication of the porous hydrogel arrays

The porous hydrogel arrays were fabricated using PEGDA hydrogel to negatively replicate a PDMS microcolumn template. In brief, 30 wt% PEGDA and 1 wt% HMPP were dissolved in deionized water by shocking for 3 min. Then, the mixed pre-gel solution was pipetted onto the PDMS template and placed in a vacuum for 8 min to fully fill the cavities. The mixed pre-gel solution was solidified by ultraviolet (UV) irradiation for 17 s. Finally, the porous hydrogel arrays were obtained by gently stripping the PDMS template.

## Cell culture

The cells were cultured in DMEM consisting of 10% FBS and 1% penicillin/streptomycin in an incubator (Thermo Fisher Scientific, USA) at 37 °C with 5% $CO_2$. The porous hydrogel arrays were sterilized under UV light for 4 hours and then placed into a 6-well plate. For the formation of cell spheroids, a cell suspension with a concentration of $2\times10^5$ cells/mL was pipetted onto the porous hydrogel arrays and cultured for 5 days. The medium was changed daily. After 5 days of cultivation, the generated cell spheroids were co-stained with 5 μM calcein-AM and 2 μM PI for 1 hour at 37 °C in the dark and then rinsed with PBS for observation.

## Establishment of drug-resistant cells

Huh7R cells were established by continuous exposure to progressively increasing doses of Lenvatinib from 100 nM to 60 μM over a period of 8 months. In brief, Huh7 cells were incubated in a 60 mm cell culture dish for 24 hours and treated with Lenvatinib for 48 hours. Then, the supernatant containing the drug was removed and replaced with fresh medium until passage. The same operation was repeated 3 times at each drug concentration, and then the cells were continually induced by increasing the drug concentration. By the end of the eighth month, the Huh7 cells obtained stable resistance and grew well in a medium containing 60 μM Lenvatinib—these cells were renamed as Huh7R cells.

## Cell viability assay

The biocompatibility of PEGDA hydrogel was evaluated by MTT assay. For the MTT assay, different concentrations (10%, 20%, and 30%, v/v) of PEGDA hydrogel films were co-cultured with Huh7 cells, and cell viability was determined on day 1, 3, and 5. Simply put, the cells were cultured in 96-well plates, and a 10% MTT solution was added to the medium and incubated at 37 °C for 4 hours. Then the medium was removed, and 150 μL DMSO was added for 10 min. Finally, the absorbance was measured at 490 nm using a microplate reader (Thermo Fisher Scientific, USA).

The viability of Huh7 and Huh7R cells ($1.5\times10^3$ per well) cultured in 2D and 3D models was tested by CCK-8. In brief, the cells were collected and cultured in 96-well plates. After 24 hours of culture, the cells were treated with increasing doses of Lenvatinib (0–64 μM) for 48 hours. Then, 10% CCK-8 was performed to measure cell viability. The OD value at 492 nm was read on the microplate reader. The $IC_{50}$ value was calculated by *GraphPad Prism*® software.

## Transwell assay

The migration ability of cells in 2D and 3D models was measured by transwell assay. Cells ($2\times10^5$ per well) in both the 2D and 3D models were digested with trypsin and then seeded into the upper chambers of transwell, and a medium containing 20% FBS was added into the lower transwell chamber. After culturing for 48 hours, the cells were fixed with 4% paraformaldehyde and stained with 0.1% crystal

violet. The migrated cell numbers were counted and analyzed by randomly selecting three different fields.

### Protein extraction and western blotting

2D cells were directly lysed by scraping into the lysis buffer. 3D cell spheroids were digested with 2 mL trypsin for 15 min and blown strongly after adding 2 mL DMEM consisting of 10% FBS. The collected cell spheroids were washed once with ice-cold PBS and immediately lysed with an RIPA buffer containing SDS, DTT, phosphatase, and protease inhibitors on ice for 50 min. The cell lysates were then centrifuged at 12,000 g for 15 min at 4 °C, and supernatant (protein extracts) was extracted. The protein content was determined by the BCA protein assay kit. Then, all the proteins were separated on 8% SDS-PAGE and electrotransferred to the PVDF membrane. Each membrane was probed with primary antibodies and then incubated with secondary antibodies. After being washed three times with TBST, each blot was quantified using the ECL reagent, and then imaging was acquired using a chemiluminescence imaging system (Analytik Jena, Germany).

### Characteristics

Images of the porous hydrogel arrays were taken with an optical microscope (Optec BDS400). The microstructures of the porous hydrogel arrays were characterized by scanning electron microscopy (SEM, Hitachi SU8010). The cell spheroids were observed by optical microscope and fluorescence microscope (Olympus SZX-16). The 3D structure of cell spheroids was taken by laser scanning confocal microscope (CLSM, Nikon A1).

## Statistical analyses

All quantitative data were expressed as means±standard deviations. Unpaired Student's *t* tests were used to denote statistical significance, and *p* values of less than 0.05 were considered statistically significant. All data were analyzed with *GraphPad Prism*® software.

## Results and discussion

In a typical experiment, the porous hydrogel arrays were generated by negatively replicating the PDMS microcolumn template, as described in Fig. 2a. In this process, the PEGDA pre-gel solution was first infused into the PDMS microcolumn template with the aid of a vacuum pump and then polymerized by UV irradiation. To obtain the porous hydrogel arrays with superior performance, the concentration of

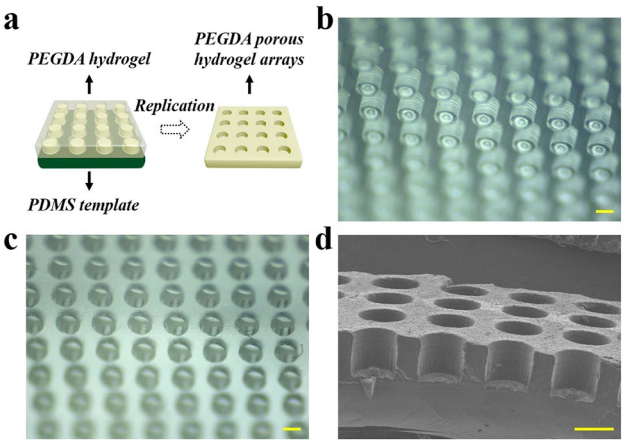


**Fig. 2** Characterization of the porous hydrogel arrays: **a** scheme of the fabrication of the porous hydrogel arrays, **b** optical image of the PDMS microcolumn template, **c** optical image of the porous hydrogel arrays, **d** SEM image of the porous hydrogel arrays. The scale bars are 200 μm

PEGDA hydrogel was optimized. For this purpose, a series of PEGDA hydrogel solutions with different concentrations (10%, 20%, and 30%, v/v) were prepared. The results show that the mechanical strength of PEGDA hydrogel increased with the increase of hydrogel concentration, while shrinkage decreased gradually (Fig. S1). Thus, in the end, a concentration of 30% was chosen for subsequent experiments. Based on the above methods, the prepared porous hydrogel arrays were studied as described in Fig. 2. Ascribed to the elaborated microcolumn structure of the template, the porous hydrogel arrays replicated from the PDMS template possessed an identical uniform and ordered pore structure, which facilitated the uniform distribution of cells into the pores (Figs. 2b and 2c). In addition, from the side view of the porous arrays under SEM in Fig. 2d, it was observed that the porous hydrogel arrays presented structural stability and uniform pore size, laying a solid foundation for further biological application.

Because the PEGDA hydrogel possesses anti-adhesive properties and excellent biocompatibility, we expected it to be well designed for culturing cell spheroids. To evaluate the biocompatibility of our prepared PEGDA hydrogel, different concentrations of PEGDA hydrogel films were co-cultured with the hepatoma cell line (Huh7 cells), and then the cell viability of the Huh7 cells was analyzed by MTT assay—a convenient way for assessing cell viability. The results indicate that the Huh7 cells grow well and proliferate in the presence of PEGDA hydrogel films after five days of culture, as shown in Fig. S2. Because of the uniform pore structure of the fabricated porous hydrogel arrays, the Huh7 cells could distribute evenly in the pores and form cell spheroids. To optimize the size of the cell spheroids, various concentrations of Huh7 cells were seeded into the porous hydrogel

arrays, and the formation of cell spheroids was observed (Fig. S3). It was found that cell spheroids could not form when the concentration of Huh7 cells was too low, while growth space and nutrient supply were limited when it was too high (Figs. S3a–S3f). Hence, a concentration of Huh7 cells at $2\times10^5$ cells/mL was chosen in subsequent investigations to give the best cell spheroid formation ability (Fig. S3d).

Based on the above-optimized experimental conditions, the hepatoma cell spheroids were fabricated in the porous hydrogel arrays. As shown in Fig. S4, we found that the hepatoma cells gradually aggregated with increased incubation times, and the cell spheroids were produced over a period of five days. Thus, the fifth day was chosen for subsequent research on resistance. In order to further verify their 3D structure, these cell spheroids were observed using a fluorescence microscope, CLSM, and SEM (Fig. 3). The results show that the generated cell spheroids had uniform size and good integrity, which was primarily attributed to the uniform pores designed in our porous hydrogel arrays being beneficial to the enrichment and equal distribution of cells in each pore (Figs. 3a–3g). In addition, these pores' design could reduce fluid-induced shear stress on cell spheroids and locate these spheroids at a particular location. In addition, the cell morphology of cell spheroids formed in the porous hydrogel arrays was significantly different from that of traditional 2D cell culture. Generally, in 2D cell culture, the cells are adherent to the flat, multi-well plates and have extended antennas. However, individual cells aggregated gradually in our porous hydrogel arrays, eventually forming a nearly perfect spherical shape with a smooth surface, which was much more similar to the morphology of solid tumors in vivo (Fig. S4 and Movie S1). Afterward, the viability of cells in the spheroids was also observed by CLSM in different Z-planes and quantified by CCK-8 assay. It was found that the cells in both the margin and the interior of the spheroids were imaged with homogeneous green fluorescence at varying locations and depths, showing that the cell spheroids cultured in the porous hydrogel arrays had high cell viability (Figs. 3h and S5). These results indicate that the generated tumor cell spheroids can potentially be an excellent model for the investigation of drug resistance

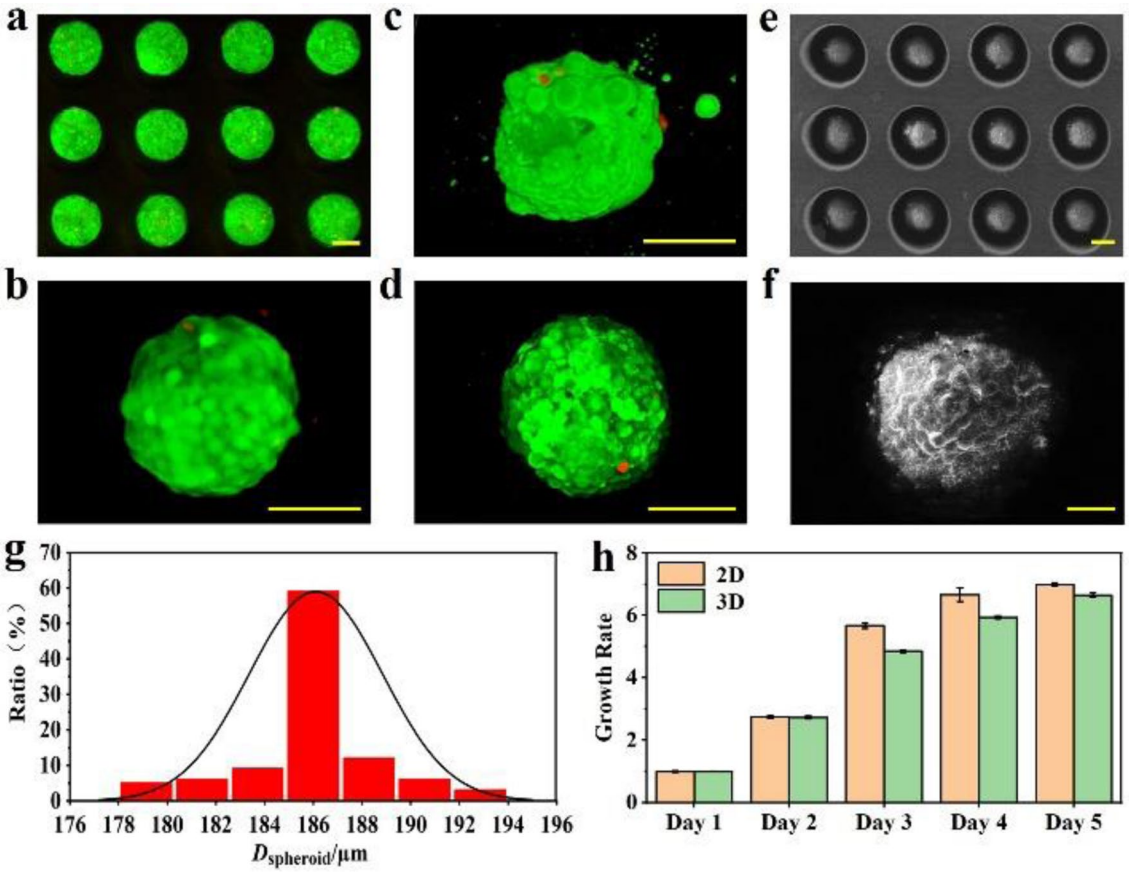


**Fig. 3** Characterization of tumor cell spheroids: **a, b** fluorescence images of tumor cell spheroids, **c, d** CLSM images of tumor cell spheroids, **e, f** SEM images of tumor cell spheroids—the scale bars are 100 μm in a–e and 25 μm in f, **g** diameter distribution of tumor cell spheroids—100 cell spheroids were analyzed, **h** the growth rate of cells in 2D and 3D culture

because they can better simulate and reconstruct the morphological, functional, and microenvironmental characteristics of solid tumors.

To exploit the application of tumor cell spheroids in drug resistance research, Lenvatinib resistant the hepatoma cell line (Huh7R cells) was first established. Lenvatinib, a type I inhibitor of tyrosine kinase, is employed for the first-line treatment of unresectable and advanced hepatocellular carcinoma (HCC) patients, displaying potent antiangiogenic activity in tumor therapy [29]. Resistance to Lenvatinib has become the main obstacle affecting the therapy of patients with advanced HCC. For which purpose, Huh7R cells were constructed in our own laboratory for 8 months. It was demonstrated that the cell viability of Huh7R cells was significantly higher than that of the parental Huh7 cells after treating with Lenvatinib for 48 hours (Fig. S6a). In addition, as described in Fig. S6b, the 50% inhibitory concentration ($IC_{50}$) value of Lenvatinib in Huh7R cells ($IC_{50}$=19.77 μM) shows that the drug resistance of Huh7R cells to Lenvatinib increased by 9.885 times compared with Huh7 cells ($IC_{50}$=2.00 μM, $p$<0.001). Further, the tumor cell spheroids of Huh7 and Huh7R cells were prepared and treated as described above (Fig. S6c). The results show that the $IC_{50}$ value of Huh7R cells ($IC_{50}$=47.09 μM) in 3D culture was significantly higher than that of Huh7 cells ($IC_{50}$=25.46 μM, $p$<0.01) (Fig. S6d)—similar to the results of 2D culture. These results indicate that the 2D and 3D models of drug resistance were successfully developed, which could be of use for subsequent research on resistance.

To confirm the feasibility and superiority of the 3D cell spheroids compared with 2D cells for resistance investigation, the Huh7 and Huh7R cells were employed for 2D and 3D culture, respectively. In this experiment, the 2D cells cultured on the culture plate and corresponding 3D cell spheroids prepared in the porous hydrogel arrays were treated with different concentrations of Lenvatinib (0–64 μM) for 48 hours and observed under fluorescence microscopy (Figs. 4a and 4b). The bright green fluorescence in living cells was stained with calcein-AM, and the red fluorescence in dead cells was stained with PI. We observed that the cells in both the culture plate and the porous hydrogel arrays gradually died as the concentration of the drug increased. However, the cells in the 3D spheroids exhibited stronger viability than those in the 2D culture at the same drug concentration, suggesting a higher level of drug resistance in 3D cell spheroids. This may be due to the 3D integrity of the

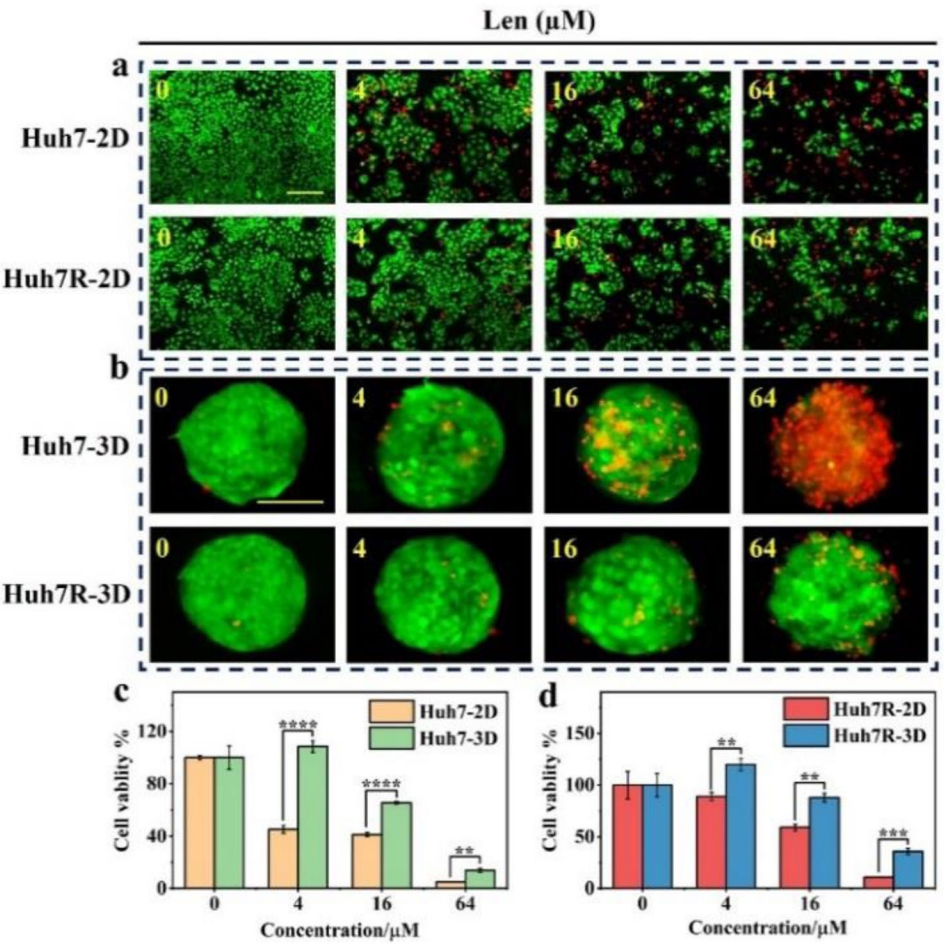


**Fig. 4** The live (green) or dead (red) cells were analyzed with the Live/Dead Viability Kit. Fluorescence images of 2D cells (**a**) and 3D cell spheroids (**b**) treated with different drug concentrations for 48 h. The cell viability of Huh7 (**c**) and Huh7R (**d**) cells in 2D and 3D models with an increased concentration of Lenvatinib (0–64 μM). $^{**}p<0.01$, $^{***}p<0.001$ and $^{****}p<0.0001$. The scale bars are 100 μm. Lenvatinib: Len

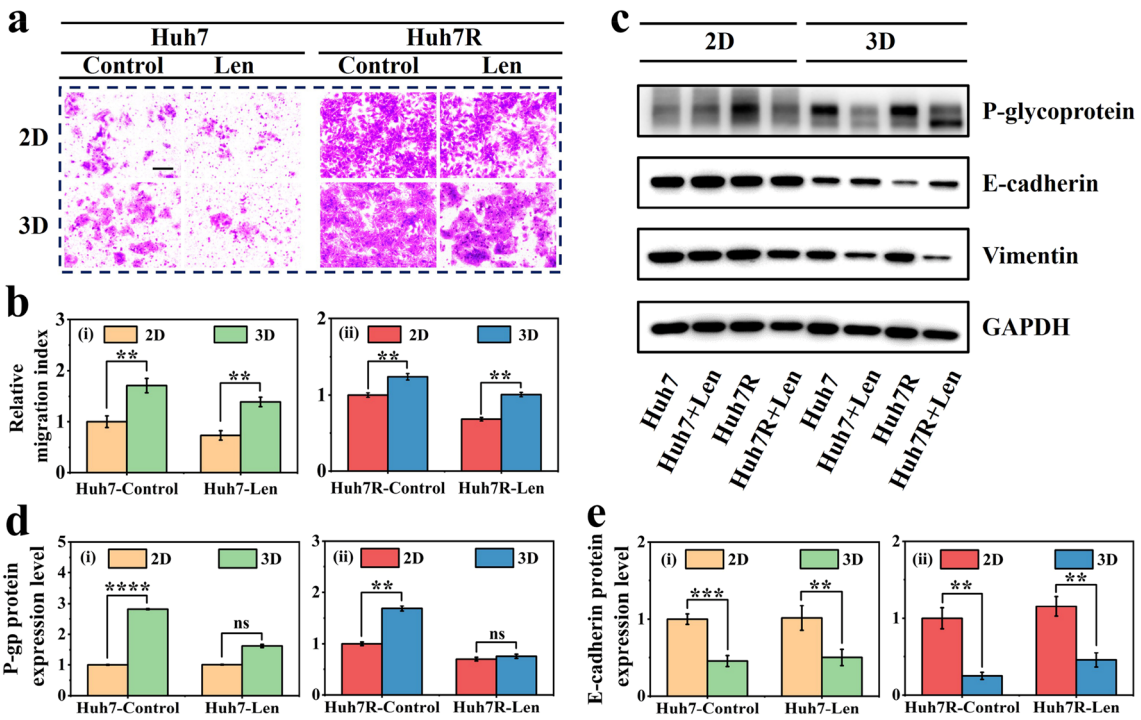


**Fig. 5** The results of cell migration ability and resistance-related protein expression in 2D and 3D models: **a** transwell assay results of migration ability in 2D cells and 3D cell spheroids with the same drug concentration, **b** the statistical results of the migration ability, **c** western blot results of the MDR- and EMT-related proteins in 2D cells and 3D cell spheroids with the same drug concentration, **d, e** the statistical results of the protein expression level. ns: not significant, $^{**}p<0.01$, $^{***}p<0.001$ and $^{****}p<0.0001$. Lenvatinib: Len

cell spheroids, making it harder for the drug to diffuse and penetrate into the central cell mass. It should be noted that although the traditional 2D model has been widely used in drug resistance research, it still cannot accurately reflect the effect of drugs in solid tumors. Therefore, the 3D cell spheroids with higher similarity to tumor tissues are considered to be more valuable models for drug resistance research.

To further verify the drug resistance effects of the 3D cell spheroids, the viability and $IC_{50}$ value of cells cultured in both 2D and 3D models were analyzed by CCK-8 assay. We demonstrated that the cells in parental hepatoma cell spheroids (Huh7-3D) were more resistant to Lenvatinib than their 2D cells (Huh7-2D) (Fig. 4c). Furthermore, cell viability was statistically different between Huh7-3D and Huh7-2D over a Lenvatinib dosing range of 0-64 μM. In particular, the $IC_{50}$ value of Huh7-3D was elevated to 25.46 μM, while it was only 2.00 μM for Huh7-2D ($p<0.001$) (Fig. S6e), which confirms that the 3D cell spheroids in the porous hydrogel arrays developed more obvious drug resistance. More importantly, the cells in the resistant hepatoma cell spheroids (Huh7R-3D) exhibited more remarkable drug resistance than the cells cultured in 2D (Huh7R-2D). We found that the cell viability of Huh7R-3D was significantly higher than that of Huh7R-2D after treatment with Lenvatinib (Fig. 4d). In addition, compared with Huh7R-2D ($IC_{50}$=19.77 μM), Huh7R-3D ($IC_{50}$=47.09 μM, $p<0.01$) showed a 2.38-fold increase in resistance to Lenvatinib (Fig. S6f), indicating that the Huh7R cells acquired higher drug resistance in 3D culture than in 2D. Taken together, the above results suggest that the 3D cell spheroids produced from both Huh7 and Huh7R cells were more resistant to Lenvatinib than 2D cells, which may affect the drug sensitivity of cells to Lenvatinib.

To explain the resistance of 2D cells and 3D cell spheroids to Lenvatinib, the cells were treated with Lenvatinib for 48 hours to detect cell migration ability and related proteins. It has been reported that the drug resistance of tumor cells may account for activating epithelial–mesenchymal transition (EMT) to gain the mesenchymal phenotype properties, including increased migration, resistance to apoptosis, and stem cells characteristics, thereby evading the effect of anticancer agents [30]. Thus, the migration ability of cells cultured in 2D and 3D cell spheroids was explored. The results show that the Huh7R-2D acquired a more significant migration phenotype compared with Huh7-2D, which also demonstrates that the drug-resistant cells we established did indeed increase migration due to obtained drug resistance (Figs. 5a and S7a). Meanwhile, the migration ability of Huh7R-3D was also significantly higher than that of Huh7-3D (Fig. S7b). In addition, compared with the corresponding 2D cells, the 3D cell spheroids had a more obvious migration

tendency, indicating that 3D cell spheroids not only acquired higher resistance to Lenvatinib but also stronger migration ability. Among these, Huh7R-3D was seen to have the most notable migratory phenotype, which is probably associated with its high drug resistance. It is worth noting that although the migration ability of 2D cells and 3D cell spheroids was inhibited after treatment with Lenvatinib, the Huh7R-2D and Huh7R-3D still maintained higher migration ability—the statistic results are shown in Fig. 5b.

In order to further explore the molecular mechanism of drug resistance in 2D and 3D models related to an increased migration phenotype, we used western blot to evaluate the changes in EMT and multidrug resistance (MDR)-related proteins. EMT is characterized by the loss of epithelial cell markers and the restoration of mesenchymal cell markers, which plays an important role in cell migration and tumor drug resistance. In addition, the expression of resistance protein P-glycoprotein (P-gp) encoded by the multidrug resistance protein 1 (MDR1) gene is correlated with cell migration. EMT signaling has been reported to simultaneously increase MDR. Targeting EMT by small molecular inhibitors might reverse MDR [31–33]. It was found that E-cadherin (an epithelial cell marker) expression decreased, while the expressions of vimentin (mesenchymal cell marker) and P-gp simultaneously increased in Huh7R-3D compared with Huh7-3D (Figs. S7c and S7d). However, only P-gp expression was improved in Huh7R-2D, and the expressions of E-cadherin and Vimentin were almost unchanged compared with that in Huh7-2D, as shown in Figs. 5c and S8. These results indicate that drug-resistant cells cultured in 2D and 3D models did develop resistance relative to the corresponding parental cells, but EMT only increased MDR in the 3D model. In addition, it was observed that the level of P-gp remarkably increased, and E-cadherin obviously decreased in the 3D model compared with the 2D model (Figs. 5d and 5e). Of even more interest, after 48 hours of Lenvatinib treatment, the expressions of P-gp and Vimentin declined and E-cadherin expression increased in the 3D model, while in the 2D model, only P-gp expression decreased, which verified the superiority of the 3D model in investigating drug resistance (Fig. S8).

## Conclusions

In summary, we have demonstrated a template replication method for fabricating porous hydrogel arrays for hepatoma cell spheroid formation and the investigation of drug resistance. Benefitting from the uniform pore structure of the porous hydrogel arrays and the strong biocompatibility of PEGDA hydrogel, hepatoma cells could form well-defined and dense 3D cell spheroids in the porous hydrogel arrays. We found that 3D cell spheroids produced from both hepatoma parental and resistant cells acquired more notable drug resistance when compared with cells in 2D culture. In addition, it was demonstrated that 3D-resistant cell spheroids were imparted with higher migratory phenotype, which was associated with the change of MDR- and EMT-related proteins in these cell spheroids. We believe that the system presented in this paper will contribute to the development of various types of 3D tissue models and provide a valuable platform for investigating drug resistance and drug testing in vitro.

**Supplementary Information** The online version contains supplementary material available at https://doi.org/10.1007/s42242-021-00141-8.

**Acknowledgements** This work was supported by the National Key Research and Development Program of China (No. 2020YFA0908200), the National Natural Science Foundation of China (Nos. 52073060, 61927805, 81974312, and 81501823), the Natural Science Foundation of Jiangsu Province (No. BE2018707), the Shenzhen Fundamental Research Program (No. JCYJ20190813152616459), the Zhejiang Provincial Natural Science Foundation of China (Nos. LY18H160049 and LQ19H160008), the Medical Scientific Research of Zhejiang Province (No. 2017KY459), Wenzhou Municipal Science and Technology Bureau (No. Y20190203), and Wenzhou Institute, University of Chinese Academy of Sciences's startup fund (No. WIUCASQD2019007).

**Author contributions** YJZ was involved in conceptualization; XL was involved in data curation analyzed, investigation, writing—original draft; XL and CMS contributed to formal analysis, validation, writing—review & editing and visualization; XS, LS, and KQS contributed to the project administration and supervision.

## Declarations

**Conflict of interest** The authors declare that they have no conflict of interest.

**Ethical approval** This article does not contain any studies with human or animal subjects performed by any of the authors.

**Consent to participate** All authors agree to participate in the work related to this article.

## References

1. Vasan N, Baselga J, Hyman DM (2019) A view on drug resistance in cancer. Nature 575:299–309. https://doi.org/10.1038/s41586-019-1730-1
2. Liu XZ, Zhang HB, Cheng RY et al (2018) An immunological electrospun scaffold for tumor cell killing and healthy tissue regeneration. Mater Horizons 5:1082–1091. https://doi.org/10.1039/c8mh00704g
3. Boumahdi S, de Sauvage FJ (2020) The great escape: tumour cell plasticity in resistance to targeted therapy. Nat Rev Drug Discov 19:39–56. https://doi.org/10.1038/s41573-019-0044-1
4. Liu J, Ye ZL, Xiang MX et al (2019) Functional extracellular vesicles engineered with lipid-grafted hyaluronic acid effectively

reverse cancer drug resistance. Biomaterials 223:119475. https://doi.org/10.1016/j.biomaterials.2019.119475
5. Zhang H, Liu YX, Chen GP et al (2020) Immunotherapeutic silk inverse opal particles for post-surgical tumor treatment. Sci Bull 65:380–388. https://doi.org/10.1016/j.scib.2019.10.023
6. Friedmann Angeli JP, Krysko DV, Conrad M (2019) Ferroptosis at the crossroads of cancer-acquired drug resistance and immune evasion. Nat Rev Cancer 19:405–414. https://doi.org/10.1038/s41568-019-0149-1
7. Liu L, Tian XH, Ma Y (2018) A versatile dynamic mussel-inspired biointerface: from specific cell behavior modulation to selective cell isolation. Angew Chem 57:7878–7882. https://doi.org/10.1002/anie.201804802
8. Li JN, Xu WG, Li D et al (2018) Locally deployable nanofiber patch for sequential drug delivery in treatment of primary and advanced orthotopic hepatomas. ACS Nano 12:6685–6699. https://doi.org/10.1021/acsnano.8b01729
9. Wang YM, Wu D, Wu GH et al (2020) Metastasis-on-a-chip mimicking the progression of kidney cancer in the liver for predicting treatment efficacy. Theranostics 10:300–311. https://doi.org/10.7150/thno.38736
10. Muraca F, Alahmari A, Giannone VA et al (2019) A three-dimensional cell culture platform for long time-scale observations of bio-nano interactions. ACS Nano 13:13524–13536. https://doi.org/10.1021/acsnano.9b07453
11. Hassan S, Sebastian S, Maharjan S et al (2020) Liver-on-a-chip models of fatty liver disease. Hepatology 71:733–740. https://doi.org/10.1002/hep.31106
12. Zhang HB, Cui WG, Qu XM et al (2019) Photothermal-responsive nanosized hybrid polymersome as versatile therapeutics codelivery nanovehicle for effective tumor suppression. PNAS 116:7744–7749. https://doi.org/10.1073/pnas.1817251116
13. Roberge CL, Kingsley DM, Faulkner DE (2020) Non-destructive tumor aggregate morphology and viability quantification at cellular resolution, during development and in response to drug. Acta Biomater 117:322–334. https://doi.org/10.1016/j.actbio.2020.09.042
14. Li SS, Ip CKM, Tang MYH et al (2019) Sialyl Lewis$^{x}$-P-selectin cascade mediates tumor-mesothelial adhesion in ascitic fluid shear flow. Nat Commun 1:2406. https://doi.org/10.1038/s41467-019-10334-6
15. Lee YB, Kim EM, Byun H et al (2018) Engineering spheroids potentiating cell-cell and cell-ECM interactions by self-assembly of stem cell microlayer. Biomaterials 165:105–120. https://doi.org/10.1016/j.biomaterials.2018.02.049
16. Shao CM, Liu YX, Chi JJ et al (2019) Responsive inverse opal scaffolds with biomimetic enrichment capability for cell culture. Research 2019:9783793. https://doi.org/10.34133/2019/9783793
17. Wu GH, Wu D, Lo J et al (2020) A bioartificial liver support system integrated with a DLM/GelMA-based bioengineered whole liver for prevention of hepatic encephalopathy via enhanced ammonia reduction. Biomater Sci 8:2814–2824. https://doi.org/10.1039/c9bm01879d
18. Chao YC, Shum HC (2020) Emerging aqueous two-phase systems: from fundamentals of interfaces to biomedical applications. Chem Soc Rev 49:114–142. https://doi.org/10.1039/c9cs00466a
19. Rebelo SP, Pinto C, Martins TR et al (2018) 3D–3-culture: a tool to unveil macrophage plasticity in the tumour microenvironment. Biomaterials 163:185–197. https://doi.org/10.1016/j.biomaterials.2018.02.030
20. Zhang LY, Chen KW, Zhang HY et al (2018) Microfluidic templated multicompartment microgels for 3D encapsulation and pairing of single cells. Small 14:1702955. https://doi.org/10.1002/smll.201702955
21. Zhang LC, Xiang Y, Zhang HB et al (2020) A biomimetic 3D-self-forming approach for microvascular scaffolds. Adv Sci 7:1903553. https://doi.org/10.1002/advs.201903553
22. Hortelão AC, Carrascosa R, Murillo-Cremaes N et al (2019) Targeting 3D bladder cancer spheroids with urease-powered nanomotors. ACS Nano 13:429–439. https://doi.org/10.1021/acsnano.8b06610
23. Li WC, Liu XB, Deng ZS et al (2019) Tough bonding, on-demand debonding, and facile rebonding between hydrogels and diverse metal surfaces. Adv Mater 31:e1904732. https://doi.org/10.1002/adma.201904732
24. Cai YL, Wu FY, Yu YR et al (2019) Porous scaffolds from droplet microfluidics for prevention of intrauterine adhesion. Acta Biomater 84:222–230. https://doi.org/10.1016/j.actbio.2018.11.016
25. Sun XM, Zhang HB, He JL et al (2018) Adjustable hardness of hydrogel for promoting vascularization and maintaining sternness of stem cells in skin flap regeneration. Appl Mater Today 13:54–63. https://doi.org/10.1016/j.apmt.2018.08.007
26. An CF, Liu WJ, Zhang Y et al (2020) Continuous microfluidic encapsulation of single mesenchymal stem cells using alginate microgels as injectable fillers for bone regeneration. Acta Biomater 111:181–196. https://doi.org/10.1016/j.actbio.2020.05.024
27. Chen KW, Fen YYF, Zhang Y et al (2019) Entanglement-driven adhesion, self-healing, and high stretchability of double-network PEG-based hydrogels. ACS Appl Mater Interf 11:36458–36468. https://doi.org/10.1021/acsami.9b14348
28. Shao CM, Chi JJ, Zhang H et al (2020) Development of cell spheroids by advanced technologies. Adv Mater Technol 5:2000183. https://doi.org/10.1002/admt.202000183
29. Faivre S, Rimassa L, Finn RS (2020) Molecular therapies for HCC: looking outside the box. J Hepatol 72:342–352. https://doi.org/10.1016/j.jhep.2019.09.010
30. Stemmler MP, Eccles RL, Brabletz S (2019) Non-redundant functions of EMT transcription factors. Nat Cell Biol 21:102–112. https://doi.org/10.1038/s41556-018-0196-y
31. Wang L, Chang Y, Feng YL (2019) Nitric oxide stimulated programmable drug release of nanosystem for multidrug resistance cancer therapy. Nano Lett 19:6800–6811. https://doi.org/10.1021/acs.nanolett.9b01869
32. Dastvan R, Mishra S, Peskova YB et al (2019) Mechanism of allosteric modulation of p-glycoprotein by transport substrates and inhibitors. Science 364:689–692. https://doi.org/10.1126/science.aav9406
33. Erin N, Grahovac J, Brozovic A et al (2020) Tumor microenvironment and epithelial mesenchymal transition as targets to overcome tumor multidrug resistance. Drug Resist Updat 53:100715. https://doi.org/10.1016/j.drup.2020.100715